Scattering from Polydisperse Melts

Marshall Fixman

Department of Chemistry, Colorado State University, Fort Collins, Colorado 80523

Received February 22, 2004; Revised Manuscript Received June 20, 2004

ABSTRACT: Effective isotropic pair potentials for polymer chains in a melt are derived from a phenomenological, coarse grained model of mixing on small distance scales, and the radial distribution functions of chain centers of mass and the scattering are calculated in the hypernetted chain approximation. The systems chosen for illustrative calculations are quasi-binary melts of deuterated and protonated polyethylene and polystyrene, both of which have been reported to exhibit anomalous composition dependence of neutron scattering. Quite large deviations from the Flory−Huggins picture of random spatial mixing of chains are found and the deviations decrease rather slowly with increasing molecular weights. However, nonrandom mixing gives rise to anomalous scattering of significant magnitude only if the mixture is asymmetric in particular ways. Differences in molecular weight (smaller for the deuterated polymer) and polydispersity (larger for the deuterated polymer) of about 10% are sufficient to exhibit anomalous scattering due to errors in the Flory−Huggins entropy of mixing. Smaller differences in the packing energies of the two different monomers, which are associated in the phenomenological model with composition dependent partial monomer volumes, reveal errors in the usual random phase analysis of scattering. Relative volumes of mixing deuterated and protonated polymer must range up to 1% in order to rationalize experimental anomalous scattering.

I. Introduction

Neutron scattering from ostensibly simple polymer melts, such as binary mixtures of natural and deuterated polyethylene (hPE and dPE, respectively), shows large discrepancies between theory and experiment which have been ascribed variously to deficiencies in one or the other.[1−3] Melenkevitz et al.[3] supported the Flory−Huggins theory on the basis of its agreement with more sophisticated calculations and concluded that the discrepancies resulted primarily from experimental error. In the present work effective pair potentials are derived from a phenomenological, coarse grained model of mixing on small distance scales, and numerical results are reported for the radial distribution functions $g_{su}(r)$ of chain centers of mass. The calculated scattering for mixtures of hPE and dPE and for mixtures of hPS and dPS (natural and deuterated polystyrene), provides some grounds for reopening the discussion.

In brief summary, quite large deviations from the Flory−Huggins picture of random spatial mixing of chains are found and the deviations decrease rather slowly with increasing molecular weights. But nonrandom mixing gives rise to anomalous scattering of significant magnitude only if the mixture is asymmetric in particular ways. First, differences in molecular weight (if 10 smaller for the deuterated polymer[4]), and polydispersity (if 10% larger for the deuterated polymer), suffice to cause significant anomalies for small volume fractions f_1 of the deuterated polymer. Second, small differences in the packing energies of the two different monomers, which will be associated with volumes of mixing, can cause anomalous scattering at small and, especially, large f_1. The absence of anomalous scattering for symmetric mixtures agrees with previous results,[3] but the large anomalies observed for asymmetric mixtures are not in obvious conflict with more sophisticated calculations because none seem to have been reported for melts that are asymmetric in the prescribed ways.

The present model and calculations have advantages and disadvantages in comparison to those made and cited by Melenkevitz et al.[3] in support of Flory−Huggins theory: here only one internal degree of freedom, the radius of gyration R_g, is retained for each chain, and the (effective) bare potential energies are inferred from a phenomenological, coarse grained model of monomer interactions and depend on (some of) the thermodynamic properties of the coarse grained volume elements. The polymer chains are thereby modeled as overlapping, spherical, monomer clouds of fluctuating size. In compensation for the simplicity of the model, which takes as given that which more ambitious theories attempt to compute, there are two advantages. First, the thermodynamic properties of coarse grained volume elements differ little from those of oligomeric mixtures and need not be calculated by complex modeling and calculations; they are empirical input. Second, the $g_{su}(r)$ can be calculated by methods that are generally believed to be rather accurate for the soft pair potentials that characterize mixing on the polymeric distance scale of R_g, and are in principle equally applicable to symmetric or asymmetric mixtures of monodisperse or polydisperse polymers. Specifically, hypernetted chain (HNC) theory is used to determine the $g_{su}(r)$ from the bare potentials, and the distribution of R_g for each kind of chain is inferred from the bare potentials and the $g_{su}(r)$.

The Flory−Huggins results can be recovered for the simplest version of the present model by truncating the iterative HNC calculations of the $g_{su}(r)$ at lowest order and taking the limit of vanishing compressibility, but these turn out to be strongly conflicting conditions; a smaller compressibility gives larger deviations from random mixing that are revealed only in higher order iterations. The general model is characterized by the free energy of mixing monomers of infinitely long chains within a coarse grained volume element, and this free energy involves at least an energy exchange parameter $\chi(p)$ similar in physical meaning to the Flory−Huggins χ parameter and dependent on the pressure p. More

10.1021/ma049646s CCC: $27.50
Published on Web 10/09/2004

generally, the coarse grained free energy corresponds closely to an excess free energy of mixing in which the ideal entropy of mixing is discarded, and which may be a complex function of local composition.

In the remainder of the Introduction, we will briefly summarize the experimental anomalies, following Crist,[1,2] and then outline the point of view taken in this work and the theoretical background.

A. Anomalies. The usual interpretation of experimental[5] scattering intensities $I(q)$ vs scattering wavenumber q is based on a quantity X_{ns} defined for binary mixtures by[6]

$$X_{ns} \equiv \frac{v_0}{2}\left[\frac{1}{Z_1 f_1 v_1 Q_1^S(q)} + \frac{1}{Z_2 f_2 v_2 Q_2^S(q)} - \frac{\beta^X}{I(q)}\right] \quad (1.1)$$

$$\beta^X \equiv (\beta_1 - \beta_2)^2 \quad (1.2)$$

where the subscripts, $t = 1$ for the deuterated chains and $t = 2$ for the protonated, label both the chain types[7] and the monomers of which they are composed. v_t is the partial monomer volume of pure type t polymer, f_t is the macroscopic volume fraction, $f_2 = 1 - f_1$, Z_t is the degree of polymerization or its weight-average for polydisperse systems (quasi-binary systems[8]), β_t is related to the scattering length α_t by $\beta_t = \alpha_t/v_t$, and $v_0 \equiv (v_1 v_2)^{1/2}$. $Q_t^S(q)$ is an internal structure factor usually approximated by the Debye result for Gaussian chains and always satisfying $Q_t^S(q) \to 1$ in the limit $q \to 0$, which will be our main but not sole interest.

As defined, X_{ns} is a purely experimental quantity in the limit $q \to 0$. It acquires theoretical significance when $I(q)$ is evaluated theoretically rather than experimentally, here in the section on Scattering, all other quantities in eq 1.1 retaining their experimental significance and values. In particular, X_{ns} becomes equal to the Flory−Huggins χ parameter in the random phase or related approximations[9−11] for $I(q)$, or by the direct application[8] of Flory−Huggins thermodynamic theory to macroscopic composition fluctuations in the $q \to 0$ limit. This form of eq 1.1 is taken, with modified notation, from Balsara et al.;[12] often simpler versions are displayed[1−3] for isotopic mixtures at $q = 0$ or with $v_1 = v_2$, and occasionally more complicated forms are displayed for inhomogeneous chains,[9,10,13] but inhomogeneous chains will not be considered here.

The anomalous aspect of experimental observations is that the observed X_{ns} at $q \to 0$, for mixtures of dPE, denoted type 1, and hPE, type 2, increases considerably as f_1 becomes small,[14] and perhaps also as f_1 nears unity.[15] Crist[2] summarizes the results for X_{ns} at $q = 0$, considered as a function $X_{ns}(f_1)$ of f_1, with the statement that $X_{ns}(0.1)/X_{ns}(0.5) \simeq 1.5$, and gives estimates of the experimental errors required to accommodate the expected constant $X_{ns}(f_1)$ in the f_1 range of experimental interest. In several instances, not all, the necessary errors considerably exceed those estimated in the original papers, but probably of greater significance are two particular aspects of the comparison. First is the cumulative impact of many results with $X_{ns}(0.1)/X_{ns}(0.5) > 1$, excluding only polystyrene melts (hPS and dPS), for which the ratio is less than unity. Second is the striking and systematic dependence[2,14] of $X_{ns}(f_1)$ on the degree of polymerization for small f_1, for the system dPE/hPE. The values of $X_{ns}(0.1)/X_{ns}(0.5)$ are larger than 1.5 for small chain lengths, and smaller than 1.5 for large chain lengths.

B. Point of View. This work[16] focuses on the nonrandom mixing of polymer chains on the distance scale of R_g. The failure of random mixing in dilute solutions is well understood[1,2,17] to arise from the (typically) repulsive interaction of polymer domains. An increasingly random mixing is expected with greater overlap of these domains caused by larger volume fraction of polymer and/or increasing chain length, but neither can increase indefinitely; the systems of interest undergo phase separation with increasing chain length. How far short of the inaccessible limit real mixtures fall is a matter for quantitative calculation.

The construction of intermolecular potentials is quite different from the usual one[17] based on short ranged, pair interactions between monomer units. Instead the potentials are derived from a phenomenological free energy density that describes coarse-grained systems. The approach goes back to the 19th century in its application to spatially inhomogeneous systems, especially interfaces,[18] but this particular work is based on a more recent proposal[19] which seems never to have been implemented with numerical calculations. This is a belated follow-up in which now conventional technology is employed for the approximate calculation of radial distribution functions. The only elaboration of the original model is the addition of one fluctuating, internal degree of freedom per chain, namely the radius of gyration R_g.

Experimental errors are regarded here simply as errors in the measurement of any of the quantities that appear on the right side of eq 1.1 and are not considered further. Nor will any attention be paid to the well understood, positive divergence of X_{ns} at the extremes of composition for systems with finite compressibility. The latter causes $1/I(0)$ to remain finite while the entropic terms in eq 1.1 diverge as $f_1 \to 0$ or $f_1 \to 1$; this divergence is virtually invisible within the f_1 range of common experimental study, e.g., $0.05 \le f_1 \le 0.95$. On the other hand, considerable attention will be paid to the divergence of X_{ns} due to asymmetries in packing energy, which may be either positive or negative unlike the divergence due to nonvanishing $I(0)$. Asymmetries in packing energy are associated here with significant volumes of mixing and in fact the former may be ascribed to the latter in this work, given the phenomenological construction of potential energies. Significant volumes of mixing, or more precisely, composition dependent partial monomer volumes, can have an effect on X_{ns} which is large, well understood in principle,[20,21] and which has little bearing on the Flory−Huggins entropy of mixing. However, there seem to have been no quantitative studies, either experimental or theoretical, of both volumes of mixing and scattering vs f_1, for the same systems and under the same conditions, and therefore their connection will be considered. Only a few studies[22−24] report volumes of mixing, and none relate them to scattering anomalies.[25]

1. Related Theoretical Work. The simulation of monomer cloud models retaining all three moments of the monomer distribution, rather than just R_g, and based on different methods for the determination of intermolecular potentials, has been reported.[26−28] Löwen et al.[29] have applied the HNC approximation, as well as simulations and still more refined closure approximations, to the study of the Gaussian core model of pair potentials, mainly for the study of liquid−solid-phase transitions. Their main conclusion relevant to the

present work is a reaffirmation of the HNC closure approximation for soft pair potentials in systems of high density. The first of a set of papers by Fredrickson et al.,[30−32] has a different sort of connection, in that it employs a similar phenomenological model of monomer density fluctuations, but then moves on to the random phase approximation and incompressibility conditions.

Melenkevitz et al.[3] should be consulted for an analysis of the applicability of many other theoretical calculations (PRISM, OCT, lattice models), to the questions addressed here, and the conclusion that they predict negligible scattering anomalies. Other recent work[33−43] will provide an entry into the many lines of investigation that have been pursued in the study of melt thermodynamics. As previously noted, none of these works report scattering calculations for systems with chain length and polydispersity asymmetry, and direct comparison with the present results for such systems is not possible. It is quite possible that these other methods would reveal similar effects due to the same asymmetries.

Nor is a comparison of theoretical methodologies possible because the papers cited in the preceding paragraph start with a detailed model of monomer−monomer interactions and this work starts with a coarse grained thermodynamic model. In principle the more detailed models could be used to infer the properties of coarse grained volume elements, but here these properties are introduced as empirical, input parameters. It will be seen below, in connection with the discussion of packing effects, that minor changes in the Flory−Huggins packing energy can cause major anomalies in the concentration dependence of $X_{ns}(f_1)$, but all of these anomalies can be removed by a modification of β^X that accounts for the dependence of partial monomer volumes on f_1; they may therefore be regarded, unlike anomalies due to chain length and polydispersity asymmetry, as pseudo-anomalies. The simple chain of argument used here, from a conventional generalization of the Flory−Huggins energy of interaction in a coarse grained volume element through the calculation of partial monomer volumes, packing energies, and anomalous scattering, is much more obscure in calculations based on a more fundamental picture of monomer pair interactions, largely because the intermediate stages of the calculation have a less transparent significance. The objective of the present work is not to replace more fundamental approaches but to provide a useful supplement.

We mention parenthetically the well-known and much discussed[20,21,44,45] fact that density fluctuations contribute negligibly to the scattering from polymer melts at $q = 0$. In the present work, no constraints on density fluctuations have been employed and none seem likely to be useful. One compressibility parameter κ_T^0 enters the coarse grained model, and a macroscopic compressibility κ_T emerges at the end of the calculation and turns out to be close, perhaps surprisingly close, to κ_T^0. Only for a comparison with Flory−Huggins theory is a vanishing compressibility limit examined, but as has been noted, this limit is available only for a truncated iteration of the HNC equations.

2. Cautions. Severe approximations have been made: restriction to a small number of internal states, approximations for the distribution among states, application of the HNC approximation to radial distribution functions, and Gaussian approximations for backbone statistics. Coarse grained free energy densities are sensitive to distance scale for systems in the critical region, at least in principle,[46] and here no distance scale for the coarse grained volume element is explicitly specified. The effective bare potentials are large but are largely screened in melts, and what is left to cause nonrandom mixing is a relatively small difference between large, opposing effects. Therefore, the numerical results are significant mainly as clues to further work, both theoretical and experimental; see the Discussion.

C. Outline. In the next section the effective potential energies are derived from an assumed Helmholtz free energy density $a(\phi)$ that defines a coarse grained model and depends on the local volume fractions $\phi(\mathbf{R})$. In the main text only formal properties of $a(\phi)$ are invoked; the specifically thermodynamic properties of $a(\phi)$ and their use as input parameters in the calculation are taken up in the Appendix. Because the polymer chains are modeled as spherically isotropic monomer clouds, the remaining sections on distribution functions and scattering differ little from what is used for (soft) atomic fluids.

Many details that seemed likely to divert attention from the main thread of argument have been relegated to footnotes and the Appendix. The reader who wishes to reproduce the results or to apply the algorithm to systems with different properties will be able to do so with the source code provided in the Supporting Information.[16]

II. Model and Potentials

A. Characterization of the System. The monomer types present in the system, such as deuterated or natural, are labeled by a discrete index t and likewise the possible architectures of a chain are labeled by a discrete index a that specifies such properties as the degree of polymerization and branching, if any. The monomers within any single chain are restricted to be of a single type t.The combined index $c \equiv (a, t)$ is a discrete and fixed property of each chain.

Individual chains are numbered by an index λ and the configurational state of a chain λ is specified by a set of coordinates $\mathscr{R}_\lambda \equiv (\mathbf{R}_\lambda, i_\lambda)$ that includes the center of mass $\mathbf{R}_\lambda$ and as many variables i_λ as are chosen to specify its internal conformation. In this preliminary work only the radius of gyration $R_{g\lambda}$ has been retained in the description of internal states, and only a discrete set of $R_{g\lambda}$ has been allowed, typically only three values. The exploration of more general options will be considered in the Discussion.

For an equilibrium calculation it is possible and useful to move the internal coordinate i_λ from the set $\mathscr{R}_\lambda$ to a set of species indices $s \equiv (i, c) \equiv (i, a, t)$, as if the internal state i of a chain were as permanent a property as its architecture a and chemical type t. This procedure is obviously useful, because it allows a quite pedestrian calculation of the radial distributions; the system now contains only invariant species. The species are here spherically isotropic chains that are present in limited variety and number. Typically the HNC equations must be solved for 12 species, stemming from two chemical types (deuterated or natural), two architectures (two different degrees of polymerization accounting for polydispersity), and three internal states (the different R_g), but the number is limited only by computational resources.

The safety of the procedure just described is not quite so obvious, because the use of invariant species seems

to imply that the internal state of a chain is an invariant of motion. Fortunately, implications for dynamics need not, and should not, be drawn from an equilibrium calculation. In an equilibrium treatment of chains, each of which has a finite number of internal states, the number of chains in each internal state will be infinite in the thermodynamic limit, the relative fluctuation in the number of chains in each internal state will vanish even if fluctuations are allowed, and therefore the numbers of all species can be constrained. Interactions between chains will indeed affect the generic distributions of chains among their available internal states, and these distributions must depend on the relative spatial configuration of chains and on their internal states, i.e., on the $\mathbf{R}_\lambda$ and i_λ. Such variations are not excluded by the modified notation and will be taken into account. The obvious difference between the indices i and c, the former starting off as a pointer to the fluctuating state of a molecule and the latter to a permanent characteristic, restricts this modified notation to the description of either specific configurations or generic distribution functions such as the singlet number densities Γ_s of species s and their volume fractions φ_s

$$\Gamma_s \equiv \frac{N_s}{V} \tag{2.1}$$

$$\varphi_s = \Gamma_s v_s Z_s \tag{2.2}$$

Here V is the (macroscopic) volume of the system, N_s is the number of chains assigned to species s, Z_s is their degree of polymerization, v_s the volume of their monomer units, and $1 \le s \le S$. Because v_s is defined as a monomer volume for a pure polymer rather than a partial monomer volume $\bar{v}_s$ in the mixture, the sum $\Sigma_s \varphi_s$ need not be unity and the φ_s are not true fractions.

It should be remarked that the above notation implies a more general dependence on the φ_s, $1 \le s \le S$, than is actually contemplated or allowed in the algorithm. At most two monomer types $t = 1, 2$ are allowed, but the number of species S may be arbitrarily large in order to account for different architectures and internal conformations. A brief summary of the distinction between input volume fractions f_t and other measures of composition is probably useful at this point.

Let $n_t = N_t Z_t$ be the number of monomers of type t in V and let V^0 be the volume of the pure polymers that compose the mixture,

$$V^0 \equiv \sum_t n_t v_t \tag{2.3}$$

Then[7]

$$f_t \equiv \frac{n_t v_t}{V^0} \tag{2.4}$$

$$\varphi_t = \sum_{s \in t} \varphi_s \tag{2.5}$$

where the notation $s \in t$ means that the values of s are restricted to those species s differing in (i, a) but belonging to the same type t. The v_s are input parameters and are restricted to have the same values, namely v_t, for all $s \in t$, so

$$\varphi_t = \frac{n_t v_t}{V} = F_v f_t \tag{2.6}$$

where

$$F_v \equiv \frac{V^0}{V} \tag{2.7}$$

$$V \equiv \sum_s n_s \bar{v}_s \tag{2.8}$$

Another set of input parameters $x_a(t)$ is relevant to the present discussion. The product $n(c) = x_a(t) n_t$ gives the number of monomers of type t available to chain architectures of type a, which differ in the illustrative calculations only in chain length $Z(c) = Z_a(t)$, where c designates the combined architecture and type indices. Thus, the $x_a(t)$ determine the polydispersity.

The singlet densities Γ_s and the φ_s have to be calculated by a cyclic iteration process because neither the relative occupancies of different internal states or the $\bar{v}_s$ are known a priori, but in terms of the Γ_s the modern apparatus for the calculation of approximate pair distributions becomes available for unmodified use. Likewise for a specific configuration, each chain λ may be characterized by its value of s and reference to a formal mapping $s = \mu(\lambda)$ will prove useful in algebraic manipulations.

B. Partition Function and Coarse Graining. A preliminary integration over all chain coordinates not contained in the sets $\mathscr{R}_\lambda$ allows the configurational integral Q in an (N, V, T) ensemble to be written in the form

$$Q = \int \exp[-\beta E_x] \, \mathrm{d}\{\mathscr{R}\} \tag{2.9}$$

where $\beta \equiv 1/k_B T$, E_x is a function of the set $\{\mathscr{R}\}$ of all $\mathscr{R}_\lambda$, and $\exp[-\beta E_x]$ is an unnormalized probability density for the set $\{\mathscr{R}\}$. If all chain coordinates were present in $\{\mathscr{R}\}$ then E_x would have the form

$$E_x = E_b + E_\phi \tag{2.10}$$

where E_b is a sum of functions of i_λ, such as the set of all bond lengths and angles of chain λ, and E_ϕ is a potential energy arising from the pair interaction of monomers, whether belonging to the same polymer chain or different ones. Here i_λ represents only the radius of gyration of λ but a formal division of E_x is still possible; $\exp[-\beta E_b]$ is an unnormalized probability for the radii of gyration of noninteracting chains and E_ϕ is what remains of the free energy of a system with constrained centers of mass and radii of gyration after subtraction of E_b. We simply assume that E_ϕ can be approximated as the integral of a Helmholtz free energy density $a(\phi)$

$$E_\phi = \int_V a(\phi) d\mathbf{R} \tag{2.11}$$

where $a(\phi)$ is assumed to depend smoothly on local volume fractions $\phi(\mathbf{R}) \equiv \{\phi_1(\mathbf{R}), \ldots, \phi_S(\mathbf{R})\}$ of the different monomer species that may be present at a point $\mathbf{R}$. By definition

$$\phi_s(\mathbf{R}) = v_s \rho_s(\mathbf{R}) \tag{2.12}$$

where $\rho_s(\mathbf{R})$ is the local monomer number density of species s. In practice, $a(\phi)$ is presumed to depend only

on partial sums of the $\phi_s(\mathbf{R})$ over all values of s corresponding to a single monomer type $t = 1, 2$. Furthermore, the v_s are defined to be functions of the ensemble temperature and density or pressure, and do not depend on $\mathbf{R}$ no matter how extreme the conditions at $\mathbf{R}$ might be.

A dependence of E_ϕ on gradients of ϕ or other terms arising from functional integrals that replace molecular coordinates, usually appears in field-theoretic treatments[47] of phase equilibria, segregation, or interfaces, but this addition is presumed to be unnecessary here on the grounds that an explicit retention of chain coordinates $\{\mathscr{R}\}$ is contemplated rather than a field theory of $\phi(\mathbf{R})$. $\phi_s(\mathbf{R})$ is defined above as the local number density of species s monomers multiplied by a constant, namely v_s, which is independent of the local or macroscopic composition.

The local fluctuations of $\phi_s(R)$ around its macroscopic average φ_s

$$\delta_s(\mathbf{R}) \equiv \phi_s(\mathbf{R}) - \varphi_s \tag{2.13}$$

are assumed to be everywhere sufficiently small that a Taylor series expansion of the free energy density $a(\phi)$ converges and can be truncated after the quadratic terms displayed,

$$a(\phi) \simeq a(\varphi) + \sum_s a_s\delta_s(\mathbf{R}) + \frac{1}{2}\sum_{s,\,u} a_{su}\delta_s(\mathbf{R})\delta_s(\mathbf{R}) + \ldots \tag{2.14}$$

It follows that $a_s = \partial a/\partial\phi_s$ is proportional to a local chemical potential μ_s and the second derivatives a_{su} are closely related to (inverse) compressibilities, but the full thermodynamic analysis of $a(\varphi)$ and the description of input parameters are relegated to the Appendix. We pause here only to introduce sufficient notation to derive the consequences of eq 2.14.

For the systems of special interest in which the polymer species differ only through isotopic substitution, there are only two monomer types no matter how large the molecular weight heterogeneity, and there are only three independent values of the S^2 matrix elements a_{su}, because $a_{su} = a_{us}$. Furthermore, all matrix elements a_{su} should have about the same large value for isotopic mixtures. The definitions and a thermodynamic estimate of the second derivative for a one component melt with $v_0 \equiv v_1$ give

$$v_0 \equiv (v_1 v_2)^{1/2} \tag{2.15}$$

$$\epsilon_{su} \equiv \frac{v_0}{k_B T} a_{su} \simeq \epsilon_0 \tag{2.16}$$

$$\epsilon_0 \equiv \frac{v_0}{k_B T \kappa_T^0} \tag{2.17}$$

and values of ϵ_0 range from 5 to 50, supposing that the nominal compressibility κ_T^0 is about 10^{-9} Pa^{-1}. Because the ϵ_{su} are large, the small differences between different ϵ_{su} play a very large role in thermodynamic properties such as phase transitions and composition fluctuations, and these differences have to be determined empirically in the phenomenological approach. The parameter definitions initiated with eq 19 will be continued below and related to the thermodynamic properties of the coarse grained volume element in the Appendix.

C. Inference of the Potentials. Equations 2.11−2.14 give

$$E_\phi = E_\varphi{}^0 + \frac{1}{2}\sum_{s,u} a_{su} v_s v_u \int \rho_s(\mathbf{R})\rho_u(\mathbf{R})\, d\mathbf{R} \tag{2.18}$$

where

$$E_\varphi{}^0 = V\left[a(\varphi) + \frac{1}{2}\sum_{s,u} a_{su}\varphi_s\varphi_u\right] \tag{2.19}$$

In the remaining analysis $E_\varphi{}^0$ plays no significant role. Radial distribution functions $g_{su}(r)$, partial structure factors, and a few thermodynamic quantities such as κ_T and the $\bar{v}_s$, namely those that may be calculated from the $g_{su}(r)$ and do not require consideration of the temperature dependence of the free energy, are inferred from the fluctuating effective energy $E_\phi - E_\varphi{}^0$ and its dependence on the configuration of the chains; these calculations do not involve $E_\varphi{}^0$.

The monomer number density of species s receives contributions from all polymer chains of that species

$$\rho_s(\mathbf{R}) = \sum_\lambda \delta(s,\mu(\lambda))\rho^\lambda(\mathbf{R}) \tag{2.20}$$

where $\rho^\lambda(\mathbf{R})$ is the monomer density at R due to a particular chain λ, $\delta(s,\mu(\lambda))$ is a Kronecker δ-function, and $\mu(\lambda)$ is the mapping function that evaluates to the species index of chain λ. After conversion from sums over species to sums over chains with the aid of eq 2.20, eq 2.18 gives

$$E_\phi = E_\varphi{}^0 + \frac{1}{2}\sum_{\kappa,\lambda} a_{\mu(\lambda),\mu(\kappa)} v_{\mu(\lambda)} v_{\mu(\kappa)} p_{\kappa\lambda}(\mathbf{R}_{\kappa\lambda}) \tag{2.21}$$

where

$$p_{\kappa\lambda}(\mathbf{R}_{\kappa\lambda}) \equiv \int \rho^\lambda(\mathbf{R})\rho^\kappa(\mathbf{R}) d\mathbf{R} \tag{2.22}$$

and $R_{\kappa\lambda}$ is the vector distance between centers of mass of chains λ and κ. The pair function $p_{\kappa\lambda}$ will depend also on whatever internal coordinates of each chain have been reserved from the preliminary averaging. The number density $\rho^\lambda(R)$ of monomer units belonging to chain λ can be put in the form

$$\rho^\lambda(\mathbf{R}) = Z_{\mu(\lambda)} m_{\mu(\lambda)}(\mathbf{R} - \mathbf{R}_\lambda) \tag{2.23}$$

where $m_s(\mathbf{r})\, d\mathbf{r}$ is the fraction of the segments of an s chain in a volume element $d\mathbf{r}$ at distance r from the chain's center of mass, and of course $\int m_s(\mathbf{r})\, d\mathbf{r} = 1$ and $\int r^2 m_s(\mathbf{r})\, d\mathbf{r} = R_{gs}{}^2$. Then

$$p_{\kappa\lambda}(\mathbf{R}_{\kappa\lambda}) \equiv \int \rho^\lambda(\mathbf{R})\rho^\kappa(\mathbf{R})\, d\mathbf{R} \tag{2.24}$$

$$= Z_{\mu(\kappa)} Z_{\mu(\lambda)} \times \int m_{\mu(\kappa)}(\mathbf{R} - \mathbf{R}_\kappa) m_{\mu(\lambda)}(\mathbf{R} - \mathbf{R}_\lambda)\, d\mathbf{R} \tag{2.25}$$

and

$$E_\phi = E_\varphi{}^0 + \frac{1}{2}\sum_{\kappa,\lambda} u_{\kappa\lambda}(\mathbf{R}_{\kappa\lambda}) \tag{2.26}$$

where $u_{\kappa\lambda}$ is a effective potential, intermolecular or intramolecular for $\kappa \neq \lambda$ or $\kappa = \lambda$, respectively, and is

given by

$$u_{\kappa\lambda}(\mathbf{R}_{\kappa\lambda}) = a_{\mu(\kappa),\mu(\lambda)} v_{\mu(\kappa)} v_{\mu(\lambda)} Z_{\mu(\kappa)} Z_{\mu(\lambda)} \times \int m_{\mu(\kappa)}(\mathbf{R} - \mathbf{R}_\kappa) m_{\mu(\lambda)}(\mathbf{R} - \mathbf{R}_\lambda) d\mathbf{R} \quad (2.27)$$

The units of m_s and a_{su} are 1/vol and $u_{\kappa\lambda}$ is dimensionless.

A considerably less cumbersome notation can be used for the interaction of a pair of chains of species s and u with separation r between centers of mass

$$u_{su}(r) = v_{su}\epsilon_{su} Z_s Z_u \times \int m_s(\mathbf{R}') m_u(\mathbf{R}' + \mathbf{r})\, d\mathbf{R}' \quad (2.28)$$

where ϵ_{su} is dimensionless by virtue of the definitions in eq 2.16 and

$$v_{su} \equiv \frac{v_s v_u}{v_0} \quad (2.29)$$

The Fourier transforms of the monomer distribution $m_s(\mathbf{r})$ and the pair potential $u_{su}(\mathbf{r})$ are defined by

$$M_s(k) \equiv \int \exp(i\mathbf{k}\cdot\mathbf{r}) m_s(\mathbf{r})\, d\mathbf{r} \quad (2.30)$$

$$U_{su}(k) \equiv \int \exp(i\mathbf{k}\cdot\mathbf{r}) u_{su}(\mathbf{r})\, d\mathbf{r} \quad (2.31)$$

respectively. Then eq 2.28 gives

$$U_{su}(k) = v_{su}\epsilon_{su} Z_s Z_u M_s(k) M_u(k) \quad (2.32)$$

The simplified notation for u_{su} and U_{su} unfortunately obscures the applicability of the same formulas to the intramolecular potential, which is given by $^1/_2 u_{ss}(0)$ for an s-chain according to eqs 2.26 and 2.27. The dependence of both intramolecular and intermolecular potentials on intramolecular coordinates such as R_g is implicit. Because no more than two monomer types have been allowed,[48] the values of ϵ_{su} that need be considered are restricted to the independent values of a 2×2 symmetric matrix $\hat{\epsilon}$. For connection to Flory–Huggins theory, and in distinction from the more fundamental input parameters discussed in the Appendix, we define χ^{FH}, ϵ, and r_ϵ in terms of the matrix elements of $\hat{\epsilon}$ by

$$2\epsilon\chi^{FH} \equiv \hat{\epsilon}_{12}^{\,2} - \hat{\epsilon}_{11}\hat{\epsilon}_{22} \quad (2.33)$$

$$\epsilon \equiv (\hat{\epsilon}_{11}\hat{\epsilon}_{22})^{1/2} h \quad (2.34)$$

$$r_\epsilon = \left(\frac{\hat{\epsilon}_{11}}{\hat{\epsilon}_{22}}\right)^{1/2} \quad (2.35)$$

Values $r_\epsilon \neq 1$ are measures of the asymmetry in packing energy. If $r_\epsilon = 1$, it turns out that the lowest order approximate solution obtained here agrees with the Flory–Huggins approximation for X_{ns}, as will be seen below.

For Gaussian chains with uncontrained internal coordinates, $m_s(r)$ is a known[17] sum of Gaussian functions of r and the potentials $u_{\kappa\lambda}(R_{\kappa\lambda})$ and their Fourier transforms are easily computed. Very little analytical information is known about $m_s(r)$ if the radius of gyration is constrained. For large R_g the monomer density is largely plastered[17,49] on a shell of radius proportional to R_g, and binodal distributions along the long axis have often been seen in simulations of the inertia tensor.[50,51,26,27] In the present work, the unconstrained Gaussian results for $m_s(r)$ have been used with simple scaling according to the value of R_g, but molecular weight heterogeneity turns out to be important and non-Gaussian statistics might also be significant.

III. Distribution Functions

A. Singlet. In this section the species label s (or u), introduced above eq 2.1, is expanded to display the internal state index i, $s \equiv (i, c)$ or $u = (j, d)$, where the first index i (or j) designates the internal state, here just the value of R_g, and the second index c or d identifies the fixed properties which are referred to as the primary structure of a chain. Then

$$\Gamma_s = \Gamma(c) P_c(i) \quad (3.1)$$

where the number density $\Gamma(c)$ of primary structures is inferred from input parameters and the volume of mixing. $P_c(i)$ is the probability distribution of c chains among their internal states i, and is to be determined by the analysis of this section. The alternate notation $P_s \equiv P_c(i)$, referring to $s \equiv (i, c)$, will be used when it is necessary to refer to results of the preceding sections.

$P_s \equiv P_c(i)$ is evaluated from

$$P_c(i) \propto \exp[-B(i, c) - \Delta A(i, c)] \quad (3.2)$$

where $B(i, c)$ is the backbone energy inferred from the known distribution[27,52] of a chain among its possible values of R_g, and $\Delta A(i, c)$ is the sum of the internal excluded volume energy $^1/_2 u_{ss}(0)$ of a single s chain and its pair interactions $u_{su}(r)$ with other chains,

$$\Delta A(i, c) = \frac{1}{2} u_{ss}(0) + \sum\nolimits_u \Gamma_u \int u_{su}(r) g_{su}(r)\, d\mathbf{r} \quad (3.3)$$

where $g_{su}(\mathbf{r})$ is the radial distribution function for a chain of species u at a distance r from a chain s at the origin. The normalization of $P_c(i)$ is $\sum_i P_c(i) = 1$. The preceding equations determine $P_c(i)$ only implicitly and the algorithmic implementation requires a cyclic iteration process, here initiated with $\Delta A(i, c) = 0$.

B. Pair. The Ornstein–Zernike[53] equation for multicomponents defines the direct correlation function $c_{ss'}(r)$ in terms of the indirect correlation $h_{ss'}(r)$ by

$$h_{ss'}(r_{12}) = c_{ss'}(r_{12}) + \sum_u \int c_{su}(r_{13}) \Gamma_u h_{us'}(r_{32})\, d\mathbf{r}_3 \quad (3.4)$$

$$h_{ss'}(r) \equiv g_{ss'}(r) - 1 \quad (3.5)$$

where energy is measured in units of $k_B T$ and $\mathbf{r}_{ss'} \equiv \mathbf{r}_{s'} - \mathbf{r}_s$. Values of the potentials of average force

$$w_{ss'}(r) \equiv -\ln g_{ss'}(r) \quad (3.6)$$

are shown below as measures of nonrandom mixing. In Fourier/matrix notation

$$H = C + C\Gamma H \quad (3.7)$$

where H is the matrix with elements $H_{su}(q)$ and H_{su} is the Fourier transform of h_{su}

$$H_{su}(q) \equiv \int \exp(i\mathbf{q}\cdot\mathbf{r}) h_{su}(\mathbf{r})\, d\mathbf{r} \quad (3.8)$$

The matrix C is similarly defined in terms of the c_{su}, and Γ is the diagonal matrix with elements equal to Γ_s.

The application of the HNC approximation to these equations seems to be a mature technology fully described in the literature,[53−55] and details pertaining to the current application are relegated to the cited works and the source code.[16] For the comparison with Flory−Huggins theory we record here only the initialization of C used for HNC iterations and constituting the whole of the Ornstein−Zernike approximation, namely $C = -U$, where U is the matrix of intermolecular potential Fourier transforms given in eq 2.34. The corresponding initialization of H is, from eq 3.7

$$H = -(\mathbf{1} + U\Gamma)^{-1}U \tag{3.9}$$

where **1** is the unit matrix.

IV. Scattering

The scattering intensity at wavenumber q, per unit volume of observed melt, is taken to be

$$I(q) = \frac{1}{V_I}\langle|\sum_j \alpha_j \exp(i\mathbf{q}\cdot\mathbf{R}_j)|^2\rangle \tag{4.1}$$

where $\langle\rangle$ is an equilibrium average, $\mathbf{R}_j$ is the position of any monomer unit j in the system, α_j is the scattering amplitude of a single monomer, and V_I is the observed volume. Equation (4.1) is presumed to be quite conventional in principle, but the algorithmic options provided for $q > 0$ require a bit of discussion. Let $\mathbf{R}_j = \mathbf{R}_\lambda + \mathbf{r}_{l\lambda}$ where the indexing $j = (l,\lambda)$ replaces the common labeling of monomer units with separate indices for the chain λ and the monomer units l within that chain, $1 \le l \le Z_s$, $s = \mu(\lambda)$, where $\mu(\lambda)$ is here the mapping function and $\mathbf{r}_{l\lambda}$ locates monomer l relative to the center of chain λ. Then

$$I(q) = I^{(1)}(q) + I^{(2)}(q) \tag{4.2}$$

where the intramolecular and intermolecular parts, $I^{(1)}$ and $I^{(2)}$ respectively, are

$$I^{(1)} \equiv \frac{1}{V_I}\langle\sum_\lambda \alpha_\lambda{}^2[\sum_l \exp(i\mathbf{q}\cdot\mathbf{r}_{l\lambda})][\sum_n \exp(-iq\cdot\mathbf{r}_{n\lambda})]\rangle \tag{4.3}$$

$$I^{(2)} \equiv \frac{1}{V_I}\langle\sum_{\lambda\neq\nu}\alpha_\lambda\alpha_\nu\sum_{l,n}\exp(i\mathbf{R}_{\nu\lambda} + i\mathbf{w}\cdot\mathbf{r}_{l\lambda} - i\mathbf{w}\cdot\mathbf{r}_{n\nu})\rangle \tag{4.4}$$

All monomers within a single chain λ are of the same type and have the same scattering amplitude α_λ.

Conversion from sums over chains to sums over chain species, with the aid of the identity $\sum_s \delta(s,\mu(\lambda)) \equiv 1$, gives

$$I^{(1)} = \sum_s \Gamma_s \alpha_s{}^2 Z_s{}^2 Q_s^S(q) \tag{4.5}$$

where $Q_s^S(q)$ is an average of $\exp(i\mathbf{q}\cdot\mathbf{r}_{\mathrm{nl}})$ over all monomer pairs and configurations of a single chain of type s

$$Q_s^S(q) = \frac{1}{Z_s{}^2}\sum_{l,n}\langle\exp(i\mathbf{q}\cdot\mathbf{r}_{nl})\rangle \tag{4.6}$$

For Gaussian chains with most internal coordinates retained in the coarse graining, e.g., for all Rouse modes with wavenumbers somewhat less than q, then $Q_s^S(q)$ is the Debye scattering function $g_D(q^2R_{\mathrm{gs}}{}^2)$ which is abbreviated here as $Q_s^D(q)$. However, in this work, the chains have been modeled as spherical clouds of monomers, and no attempt has been made to treat correlations between $\mathbf{r}_{l\lambda}$ and $\mathbf{r}_{n\nu}$ for monomer units on either the same or different chains. A consistent implementation of the model requires use of the spherical monomer distribution $m_s(r)$ and evaluation of $Q_s^S(q)$ as the square of the Fourier transform of $m_s(r)$, that is, as $M_s{}^2(q)$. Likewise in a consistent treatment, $I^{(2)}(q)$ is given by

$$I^{(2)}(q) = \sum_{s,u} D_s D_u \alpha_s \alpha_u Z_s Z_u M_s(q) M_u(q) H_{su}(q) \tag{4.7}$$

The two functions, $Q_s^D(q)$ and $M_s{}^2(q)$, differ starting with terms of order q^4 in a power series expansion.

The algorithmic implementation allows some choice between consistency and accuracy in the evaluation of $I^{(1)}(q)$ and $I^{(2)}(q)$ from eqs 4.5 and 4.7. Option 0 is the most consistent and uses $Q_s^S(q) = M_s{}^2(q)$ in eq 4.5 and uses eq 4.7 as shown. Option 1 uses $Q_s^S(q) = Q_s^D(q)$ in eq 4.5 and eq 4.7 as shown. Option 2 uses $Q_s^S(q) = Q_s^D(q)$ in eq 4.5 and replaces $M_s(q)$ in eq 4.7 by $[Q_s^D(q)]^{1/2}$. There is little justification for option 2 in the present work, but it does result from low order approximations to scattering interference between chains in Gaussian models,[17] and from random phase and related approximations.[9−11]

It should be noted further that these options control only the evaluation of the theoretical $I(q)$ and not the definition of X_{ns} in eq 1.1. In eq 1.1, it is assumed that $Q_s^S(q) = Q_s^D(q)$ because that equation is intended to describe experimental practice; the options control only the numerical calculation of $I(q)$.

A. Two Species in the Flory—Huggins Approximation. To illustrate the connection between the more general approximations and the result obtained for random mixing of chains, analytical results are displayed here for the particular case $S = 2$ and with the HNC iterations truncated at the initialization stage. The distribution of R_{g} retains its initialized form, but that form is of little concern because the relevant Fourier transforms are independent of the distribution at $q = 0$.

With the definition

$$F_\epsilon = F_v{}^2\frac{(\beta_1 - r_\epsilon\beta_2)^2}{r_\epsilon(\beta_1 - \beta_2)^2} \tag{4.8}$$

where eq 2.7 defines $F_v = V^0/V$, one finds in the large ϵ limit after elementary but messy algebra that eqs 3.9, 4.5, and 4.7 give

$$\frac{\beta^X}{I^{\mathrm{FH}}(q)} = \frac{1}{F_\epsilon}\left[\frac{r_\epsilon{}^{-1}}{M_1{}^2 f_1 Z_1 v_1} + \frac{r_\epsilon}{M_2{}^2 f_2 Z_2 v_2} - \frac{2}{v_0}\chi^{\mathrm{FH}}\right] \tag{4.9}$$

Note the occurrence of $M_s{}^2(q)$ rather than $Q_s^D(q)$. This result corresponds to option 0 above; $M_s{}^2(q)$ would be replaced by $Q_s^D(q)$ with option 2. Option 1 has not been worked through for analytical display but the results of all three options are routinely calculated in the implementation. Equation 4.9 with an arbitrary value of r_ϵ is a generalization of the simplest Flory−Huggins approximation, a generalization which is hard to avoid in the phenomenological treatment of coarse graining. The special value $r_\epsilon = 1$ is accompanied by (or caused

by), negligible volume of mixing and $F_v = F_\epsilon = 1$; see the further discussion below. With $r_\epsilon = 1$ and option 2, eq 4.9 gives the same result as the incompressible random phase approximation, eq 1.1, with X_{ns} replaced by the Flory−Huggins χ^{FH}, namely

$$\frac{\beta^X}{I^{RP}(q)} = \left(\frac{1}{Z_1 f_1 v_1 Q_1^D(q)} + \frac{1}{Z_2 f_2 v_2 Q_2^D(q)}\right) - \frac{2}{v_0}\chi^{FH} \quad (4.10)$$

The scattering and the value of $X_{ns}(q)$ in the $q = 0$ limit of eq 4.9 are completely unaffected by the radius of gyration in the truncated iteration, and this remains true if the separate polymer types are polydisperse, because in the $q = 0$ limit the lowest iterate of H given in eq 3.9 depends only on the $q = 0$ limit of the bare potential, eq 2.32, which is independent of the monomer distribution $m_s(r)$.

In the present work the results obtained from truncation of the HNC iterations at the lowest order are designated as Flory−Huggins results for any values of ϵ, $r_\epsilon(f_1)$, and S, even though eqs 4.9 and 4.10 are valid only for $S = 2$ and $\epsilon \rightarrow \infty$, and the second equation is valid only for $r_\epsilon = 1$. Truncation of the HNC iterations might be a useful approximation for binary mixtures of deuterated and natural polymers, if both have identical or at least very similar chain lengths and architectures, because in that circumstance the failure of random mixing does not seem to produce significant scattering anomalies. The HNC iterations always seem to diverge as $\epsilon \rightarrow \infty$, but for this limited class of systems the divergence occurs with negligible change in $I(0)$ for as many successive iterates as are possible, and the dependence of $I(0)$ on the magnitude of ϵ (or κ_T^0) is rather weak.

In view of the possible utility of eq 4.9 for this limited class of systems, and in view also of the objections[1−3] leveled against modifications of the Flory−Huggins that result from lattice models with vacancies, on the grounds especially of their misbehavior at small f_1 or f_2, it might be worth while calling attention to what seems to be similar misbehavior of eq 4.9 in those small and large f_1 limits, if $r_\epsilon(f_1) \neq 1$. One might expect that eq 4.9 should agree, in those limits, with the more familiar eq 4.10. This expectation, however, does not take into account other consequences of $r_\epsilon(f_1) \neq 1$ to be described in the next section, namely that this generalization of the Flory−Huggins model can lead to a significant volume of mixing; or conversely, significant volumes of mixing may cause $r_\epsilon(f_1) \neq 1$; see the Appendix. The partial monomer volumes in the mixture, $\bar{v}_i$, then differ from the partial monomer volumes v_i of pure monomer, and the factor β^X no longer suffices[20,21] to make $\beta^X/I(q)$ independent of the scattering factors α_i or to give the expected limits. These matters will be considered further below, along with a revised β^Y that eliminates the anomaly at the expense of information that is not usually in the hands of those who analyze scattering data.

V. Results

Illustrative results are presented first for monodisperse melts of deuterated and protonated polymers, each type consisting of a single chain length which may, however, differ between types, and second for polydisperse melts, each type consisting of two different chain lengths with equal volume fractions. The significance of the phenomenological parameters is briefly summarized with two equations from the Appendix. The free energy of mixing of a coarse grained volume element V_c^0 is taken to be

$$\Delta G_m = \frac{k_B T V_c^0}{v_0} f_1 f_2 \sum_k (f_1 - f_2)^k \chi_k \quad (5.1)$$

and only two terms $k = 0, 1$ are retained in the series. Pressure derivatives of the χ_k are required for calculation of the potential energy coefficients $\hat{\epsilon}_{tt'}$, according to eq A22, and are parametrized with

$$l_k^p \equiv \frac{k_B T}{v_0}\left(\frac{\partial \chi_k}{\partial p}\right)_{T,n} \quad (5.2)$$

The bond lengths b_t in the tables enter the calculations solely through the expression $Z_t b_t^2/6$ for the mean square radius of gyration in the absence of the excluded volume free energy ΔA of eq 3.2.

Table 1. General Structural and Scattering Parameters Which Apply to All of the Monodisperse Polyethylene (PE) and Polystyrene (PS) Systems Illustrated in Figures 1−4 (PE) and 5 and 6 (PS), Respectively[a]

	$10^4\alpha_1$(D,Å)	$10^4\alpha_2$(H,Å)	v_1, v_2 (Å^3)	b_1, b_2(Å)	$10^9\kappa_T^0$ (Pa^{-1})
PE	4.00	−0.166	60	5.8	1.1
PS	10.7	2.33	165	7.0	0.5

[a] Additional parameters are given in the figure captions. Values are estimated at 160 °C for monomer units C_2H_4 (hPE) and C_8H_8 (hPS), or their deuterated substituents.

The parameter values are kept extremely simple for the monodisperse systems in order to study individual effects, and are listed in Table 1 and in the figure captions. Although all parameter sets are labeled as pertaining to either polyethylene or polystyrene, the designation is nominal for the monodisperse systems and no attempt is made to fit experimental results for particular systems. The physical significance and interpretation of the two scattering anomalies, the real anomalies due to asymmetries in chain length and the pseudo-anomalies due to packing asymmetry, will be discussed at the end of the subsection on monodisperse systems, along with the effects of allowing for a distribution of chain radii of gyration.

The more complicated parameter sets in Table 2 apply to the polydisperse systems, and are chosen to fit the experimental results of Londono et al.[14] The objective of such fits is merely to show a possible relevance of the model to experimental data on the basis of parameter values that are not (yet) known to be in gross conflict with experimental facts. Support or refutation of the model and calculations must be sought by different means, both experimental and theoretical, that are considered in the Discussion.

A. Monodisperse Systems. 1. Polyethylene. The systems in Figures 1−3 all concern small chain length melts of dPE and hPE; Z_1 and Z_2 are in the vicinity of 1000 and all input parameters χ_k and l_k^p introduced in the Appendix are set to zero. In Figure 1 for $X_{ns}(f_1)$, the solid curve decreases from 64×10^{-4} at $f_1 = 0.05$ to 1.6×10^{-4} at $f_1 = 0.95$, with $Z_1 = 700$ and $Z_2 = 1300$. If the molecular weights are reversed so that dPE has the higher Z, then the behavior of $X_{ns}(f_1)$ is also nearly reversed, as shown in the dashed curve of Figure 1. The dotted curve shows results for dPE and hPE with equal chain lengths, and $X_{ns}(f_1)$ very nearly vanishes for all

Table 2. Parameters Are Given for the Polydisperse Polyethylene (Code[16] *peh*) and Polystyrene (Code[16] *psh*) Systems Illustrated in Figures 7−9[a]

code	Z_1	Z_2	b_1	b_2	$10^4\chi_k$	l_k^p
peh/40a1	2360, 5640	3700, 5100	5.8	6.0	3.7, 0.1	0.02, 0.05
peh/40b1	2360, 5640	3400, 4600	5.8	6.0	3.7, 0.1	0.02, 0.05
psh/2b1	6000, 17000	5800, 12200	7.0	7.0	1.6, − 0.016	0, − 0.1

[a] Parameters not given here are given in Table 1. The two chain lengths for each polymer type $t = 1$ (D) and $t = 2$ (H) are present in half the macroscopic volume fraction f_t.

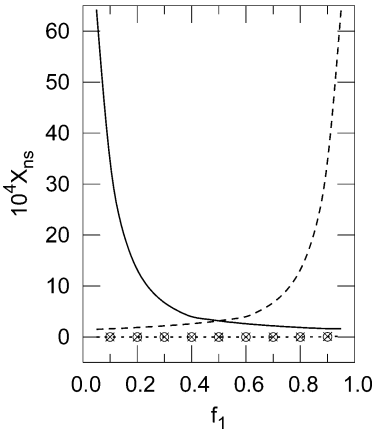

Figure 1. X_{ns} vs f_1 results are shown for three binary mixtures of dPE(1) and hPE(2), both monodisperse. For the solid curve (code[16] *pes2/10a1*), $Z_1 = 700$ and $Z_2 = 1300$. For the dashed curve (code *pes2/10b1*), $Z_1 = 1300$ and $Z_2 = 700$. For the dotted curve (code *pes2/10z1*), $Z_1 = Z_2 = 1000$. The circles and crosses are modified runs of *10a1* and *10b1*, respectively (with codes *pes2/10aFH* and *pes2/10bFH*, respectively), truncated at the lowest iteration and corresponding to the Flory−Huggins approximation. Parameter values are $\chi_k = 0$ and $l_k^p = 0$, all k. Other values are given in Table 1. All smooth curves are cubic splines passing through equally spaced points, here nineteen in number.

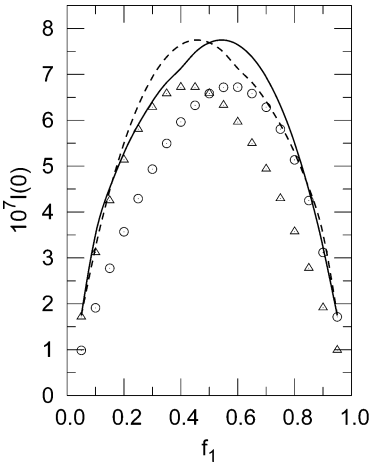

Figure 2. $I(0)$ vs f_1 is shown for the parameter code[16] sets *pes2/10a1* (solid curve) and *pes2/10b1* (dashed curve) of Figure 1. The circles (code *pes2/10aFH*) are *10a1* truncated runs corresponding to the generalized Flory−Huggins approximation, and the triangles (code *pes2/10bFH*) are *10b1* truncated runs.

f_1, as it does also if the HNC iterations are truncated at lowest order, corresponding to the Flory−Huggins approximation shown in circles and squares. Correlation holes[11] are always calculated in the algorithm[16] but are not reported here except to note that they deviate by less than a few parts in 10^3 from their nominal values of −1 for an incompressible system.[56] The algorithm[16] gives an $\langle R_g^2\rangle^{1/2}$ for system *10a1* that is about 5% greater than its Θ value at $f_1 = 0.05$ and becomes a few percent

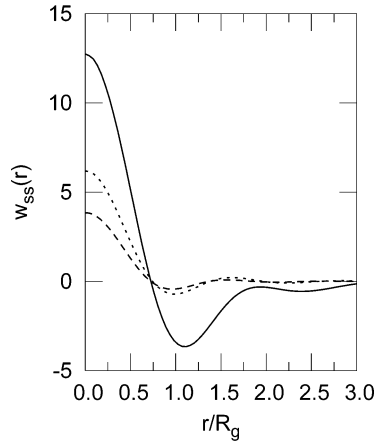

Figure 3. $w_{ss}(r)$ is the potential of average force for the interaction of two chains each of species s, in units of k_BT, and r/R_g is the separation distance relative to the radius of gyration, for the same systems illustrated in Figures 1 and 2. The solid line shows *10a1* with $s = 1$ and the dashed line shows *10a1* with $s = 4$. The dotted line shows *10z1* with $s = 1$. For all curves, $f_1 = 0.05$.

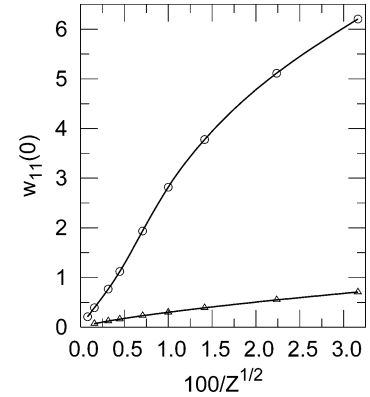

Figure 4. The *z4* data (code[16] *pes0/z4*), circles, obtained for the *10z1* system described under Figure 1, modified as follows. Here only the deuterated polymer is present, Z varies as shown in the figure, and a higher accuracy and finer grid are used for the Fourer transforms, although these are needed only at the largest Z. The *y4* data (code *pes0/y4*), triangles, differ only through exclusion of contracted and expanded R_g from the description of the internal state. The curves are cubic splines through the displayed points.

still larger at $f_1 = 0.95$. Similar but not identical expansions are found for hPE.

The scattering intensity $I(0)$ vs f_1 is shown in Figure 2 and the differences between truncated and converged iterations are seen to be much less conspicuous than they are for X_{ns}. The symmetric system with $Z_1 = Z_2 = 1000$ is not shown, but gives a symmetric plot of $I(0)$ vs f_1. Several examples of $w_{ss}(r)$, the potentials of average force, are shown in Figure 3 for both asymmetric and symmetric systems, and for the latter the very slow vanishing of $w_{ss}(0)$ with increasing Z is shown in Figure 4. Extremely large values of $w_{ss}(0)$ in Figure 3 are found for the species $s = 1$, which is the deuterated polymer,

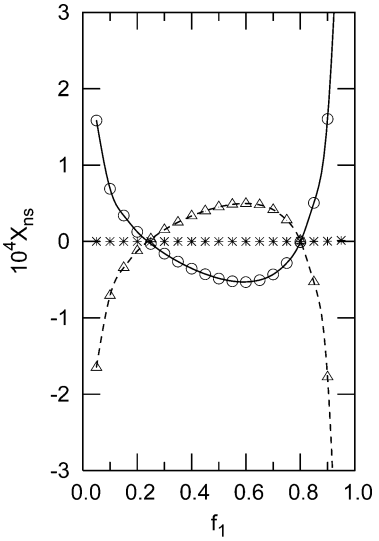

Figure 5. X_{ns} vs f_1 results are shown for three binary mixtures of dPS (1) and hPS (2), all monodisperse with $Z_1 = Z_2 = 2000$, with all $\chi_k = 0$, and differing only in their values of l_1^p; all $l_0^p = 0$. For the solid curve (code[16] *pss/2a1*) $l_1^p = 0.06$. The circles (code *pss/2aFH*) differ from the *2a1* system only in having the HNC iteration truncated at lowest order, corresponding to a generalized Flory−Huggins model. The dashed curve (code *pss/2b1*) and triangles (code *pss/2bFH*) differ only in having $l_1^p = -0.06$. The asterisks (code *pss/2c1*) differ from *2a1* systems only in having $l_1^p = 0$.

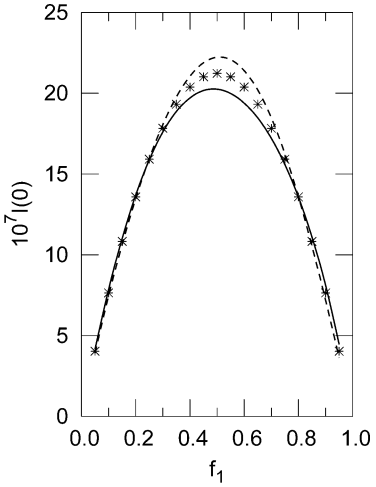

Figure 6. $I(0)$ vs f_1 for three of the systems shown in Figure 5, with the same significance for curves and symbols.

$Z_1 = 700$, in its contracted state (code[16] *pes2/10a1*). In fact, the interaction energy of this species with all other species is large and eq 3.2 reduces the singlet density of species $s = 1$ to very small values. For $s = 4$, the protonated polymer with $Z_2 = 1300$ in its contracted state, the repulsion is much less, while for the system with $Z_1 = Z_2 = 1000$ (code[16] *pes2/10z1*) the repulsion is intermediate.

Large repulsive interactions are accompanied by extensive clustering as shown in the solid curve of Figure 3, and this clustering is sufficiently large to cause a net positive value for the corresponding cluster integral $H_{ss}(0)$. Clustering of this magnitude is probably a sign of incipient phase separation, but because $\chi = 0$ the HNC equations never signal the presence of a spinodal by failing to converge for systems with the indicated degree of asymmetry in Z_1 and Z_2; further increases in the asymmetry of Z'*s* do give convergence problems.

Justification for averaging the solid and dashed curves in Figure 1, to obtain the rather symmetric $X_{ns}(f_1)$ vs f_1 curves that have been suggested[1−3,14] as characteristic of experimental data, would have to be based on a rather peculiar phase separation of polydisperse systems into domains of two types, both having the same f_1 but one having only (or mostly) long protonated and short deuterated chains, the other type having short protonated and long deuterated chains. It is not apparent that a domain structure with uniform f_1 could be recognized in neutron scattering, but neither is it apparent why it would occur.

2. Polystyrene. The input parameters are shown in Table 1 and in the figure captions. The results are shown for X_{ns} in Figure 5 and for $I(0)$ in Figure 6. The only difference between the three input data sets *10a1*, *10b1*, and *10c1* is the value of l_1^p, which is 0.06, −0.06, or 0, respectively. The nonvanishing l_1^p causes relative volumes of mixing that vanish at $f_1 = 0.5$, but rise/fall to values ±0.006 at $f_1 = 0.2$ or 0.8, and cause ratios of the packing energies $r_\epsilon(f_1)$ to reach values of 0.95 or 1.05 at the composition extremes. Values $r_\epsilon < 1$ cause a positive divergence of X_{ns} at the extremes of composition, and $r_\epsilon > 1$ causes a negative divergence. For the specified parameters the (generalized) Flory−Huggins results differ little from the HNC results carried through to convergence. The X_{ns} vs f_1 curves of Figure 5 are conspicuously asymmetric, the larger anomaly being seen at large f_1; the $I(0)$ vs f_1 curves of Figure 6 are less asymmetric. The asymmetry is due to the difference in scattering lengths α_1 and α_2 shown in Table 1 and decreases if, e.g., α_2 is increased toward the value of α_1.

If β^X in eq 1 is replaced by[20,21]

$$\beta^Y \equiv F_v^3\left(\frac{\bar{v}_1\bar{v}_2}{v_1v_2}\right)^2\left(\frac{\alpha_1}{\bar{v}_1} - \frac{\alpha_2}{\bar{v}_2}\right)^2 \qquad (5.3)$$

using the calculated values of $\bar{v}_1$ and $\bar{v}_2$, then the anomalous scattering due to $r_\epsilon(f_1) \neq 1$ disappears.[16,57] The particular form of eq 5.3 follows from scattering and fluctuation theory in the limit $q \to 0$, for example from eq 18 of Taylor et al.[20] The more general result for $q > 0$, for example eq 15 of Joanny and Benoit,[21] gives a very similar formula with $\bar{v}_t(q)$, defined in terms of cluster integrals, replacing $\bar{v}_t$ and reducing to it at $q = 0$. Calculated values of $\bar{v}_t$ for macroscopic systems do not differ significantly from those introduced in the Appendix to characterize the coarse grained volume element, nor do they differ for the compressibility. This observation is consistent with the speculation of Joanny and Benoit[21] that the q dependence of the $\bar{v}_t(q)$ is small.

3. Significance. Consider first the real scattering anomalies due to an asymmetry in chain length. According to Figure 1, the scattering anomaly due to an asymmetry in chain length is also asymmetric and is much larger if the volume fraction of the shorter chain is small rather than large. The reason for this behavior is that short chains have a greater monomer density than long chains. For Gaussian chains the maximum monomer density occurs at the center of the monomer cloud and varies as $1/\sqrt{Z}$. Moreover, mixing of polymer chains of a given type is more complete at higher volume fractions of that type than at lower volume fractions, because they can more easily avoid each other at low

volume fractions, and the combined effects of greater repulsion between shorter chains than long, due to the higher monomer density of the former, and their ability to avoid overlap at small volume fractions, gives rise to the strongly anomalous scattering for short chains at small volume fractions.

The allowance for fluctuations in the radius of gyration and the consequent shifts in $\langle R_g^2 \rangle$ from Θ values has a complicated set of consequences. The most dramatic effect is a great reduction in the probability of contracted states due to their higher monomer density. This effect is identical in its underlying cause to the effect of chain length asymmetry discussed in the preceding paragraph. If one allows different R_g species but does not allow their relative probabilities to shift according to the relative strengths of intramolecular and intermolecular excluded volume effects, then the HNC iterations become unstable just as they do for too large chain length asymmetry. However, if the probabilities are allowed to shift, then the net change in scattering intensity from the simpler model that allows only a single R_g species for each chain is generally moderate.

The pseudo-anomalies shown in Figure 5 reflect real properties of the free energy of mixing that show up in the small volume of mixing, less than 0.6% for the systems illustrated in Figure 5, and in the relative energy required to pack deuterated versus protonated monomers into the coarse grained volume element. As was noted above, the pseudo-anomalies may be eliminated by replacing the conventional β^X of eq 1.2, appropriate for theoretical models of incompressible systems, with the β^Y of eq 5.3; then all curves in Figure 5 would be indistinguishable[57] from $X_{ns} = 0$ throughout the displayed range of f_1. In this limited sense the pseudo-anomalies could be ascribed to the finite compressibility of real systems.

B. Polydisperse Systems. 1. Polyethylene. The molecular weights reported by Londono et al.[14] are mostly a few percent larger for hPE than dPE, but range from −1% to +11% larger. For one set of our runs, code[16] peh/40a1, the hPE chain lengths are taken to be 10% larger, as was true of the $N = 4400$ system that received the most extensive analysis[1−3,14] The experimental polydispersity values[14] $\langle Z_1 \rangle_{wt}/\langle Z_1 \rangle_{num}$ (type *d*) are a few percent larger than the $\langle Z_2 \rangle_{wt}/\langle Z_2 \rangle_{num}$ (type *h*) for larger chain lengths but are about the same for small chain lengths, with values near 1.1. The polydispersities used here may be inferred from Table 2 and are shown in Figure 7 caption and are discussed below.

The deuterated polymer has a larger polydispersity than the protonated polymer for codes[16] peh/40a1 and peh/40b1 of Figures 7 and 8, a value $\langle Z_1 \rangle_{wt}/\langle Z_1 \rangle_{num} = 1.202$ in comparison with 1.026 for protonated *peh/40a1* and 1.023 for protonated *peh/40b1*. If the polydispersities are matched at the value $\langle Z_t \rangle_{wt}/\langle Z_t \rangle_{num} = 1.1$ for both deuterated and protonated polymers, by shifting the two values of Z closer together for the deuterated polymer and farther apart for the protonated, leaving the $\langle Z_t \rangle_{wt}$ unchanged, then the anomalous increase in X_{ns} is reduced to very small values, about 5%, for f_1 in the range $0 \leq f_1 \leq 0.5$. But X_{ns} remains virtually unchanged for $f_1 > 0.5$. The large anomaly seen at small f_1 in Figure 1 is not matched here because the chain length asymmetry is much smaller. On the other hand, the remaining anomaly at large f_1 is due to the finite volume of mixing, which is quite asymmetric for the code *peh* parameters of Table 2, as will be illustrated below in the last figure.

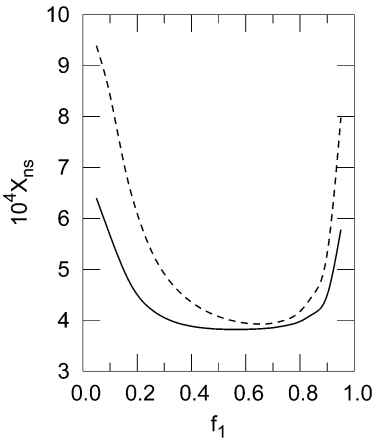

Figure 7. X_{ns} vs f_1 is shown for two of the polydisperse polyethylene systems described in Tables 1 and 2. The solid curve (code[16] *peh/40a1*) has $\langle Z_1 \rangle_{wt} = 4000$, $\langle Z_1 \rangle_{wt}/\langle Z_1 \rangle_{num} = 1.202$ and $\langle Z_2 \rangle_{wt} = 4400$, and $\langle Z_2 \rangle_{wt}/\langle Z_2 \rangle_{num} = 1.026$. The dashed curve (code *peh/20a1*) differs only in the halving of all chain lengths.

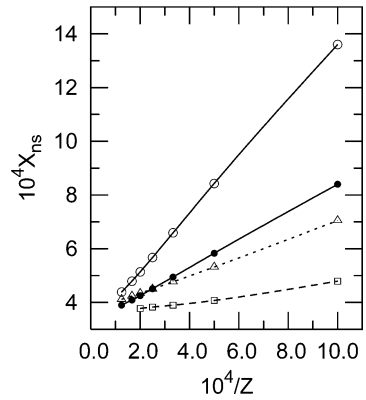

Figure 8. X_{ns} vs $1/\langle Z_1 \rangle_{wt}$ for some of the polydisperse peh systems shown in Figure 7 and Table 2, all chain lengths for codes[16] *peh/40a1* and *peh/40b1* being multiplied by the same factor. The curves are cubic splines through the displayed points. The open circles and solid curve refer to deuterated volume fraction $f_1 = 0.1$, triangles and dotted curve to $f_1 = 0.9$, and squares and dashed curve to $f_1 = 0.5$, all deriving from chain length multiples of code[16] peh/40a1. The filled circles and solid curve are based on the parameters of code *peh/40b1* with $f_1 = 0.1$; here the deuterated and protonated polymers have the same weight-average chain length in contrast to *peh/40a1*, where the protonated polymers are 10% longer than the deuterated.

For code *peh/40b1* of Table 2 and Figure 8, deuterated and natural polymers have the same $\langle Z \rangle_{wt}$ and the anomalous scattering is considerably decreased but is not absent because the asymmetry in polydispersity remains. The anomalies at large f_1 are due largely to the assumed values for the pressure derivatives l_k^p and are little affected by asymmetry in molecular weight or polydispersity. The accompanying volume of mixing will be shown below.

2. Polystyrene. The polystyrene results of Londono et al.[14] were fit with the parameters of Table 2, which agree roughly in chain length and polydispersity with those for one of their experimental systems. The molecular weight distribution is quite broad and this moderates the negative divergence of X_{ns} shown in Figure 9. The existence of a negative divergence is, however, entirely due to the large, negative l_1^p parameter, which also gives rise to the volume of mixing shown in Figure 10 for both the polyethylene and polystyrene fits.

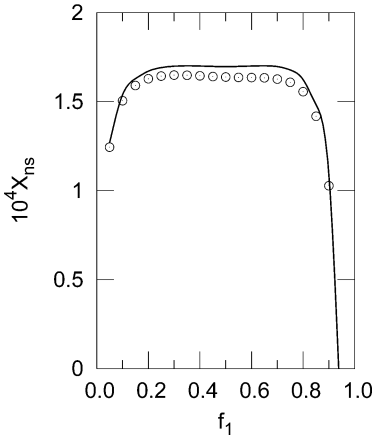

Figure 9. X_{ns} vs f_1 is shown for the polydisperse polystyrene systems described in Tables 1 and 2. The solid curve (code[16] *psh/2b1*), is a cubic spline through nineteen undisplayed points for a system with $\langle Z_1\rangle_{wt} = 1.15 \times 10^4$, $\langle Z_2\rangle_{wt} = 0.9 \times 10^4$, $\langle Z_1\rangle_{wt}/\langle Z_1\rangle_{num} = 1.30$ and $\langle Z_2\rangle_{wt}/\langle Z_2\rangle_{num} = 1.12$. The displayed points are Flory−Huggins results for the same system (first iterates of the HNC equations).

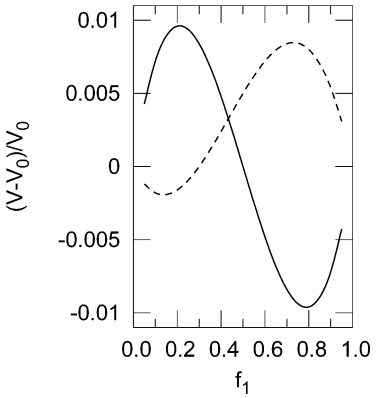

Figure 10. Relative volume of mixing for codes[16] *psh/2b1* (polystyrene, solid curve) and *peh/40a1* (polyethylene, dashed curve) with the parameter values given in Table 2. Volumes for code *peh/40b1* are not distinguishable from *peh/40a1*.

VI. Discussion

A. Results. In general there are no surprising effects on any of the results if χ_0 and χ_1 are moderately varied. If the HNC iterations converge, then X_{ns} vs f_1 curves merely shift up or down or tilt according to the changing values of χ_0 and χ_1, respectively. Of course one expects a phase transition as $\chi_0 Z$ becomes large, and the HNC iterations do indeed fail to converge as $\chi_0 Z$ becomes large. However, the more surprising effects that bear on the scattering anomalies are due to asymmetries in chain length, polydispersity, and packing energies.

1. Chain Length and Polydispersity. Scattering anomalies caused by asymmetries in chain length, polydispersity, and the use of a smaller b for deuterated than for protonated polymer are relevant primarily to polyethylene and all act through the same mechanism; the asymmetries in system parameters cause asymmetries in the radial distribution functions, for protonated vs deuterated polymers, on a distance scale of R_g. Absent these, the strong deviations from random mixing are essentially the same for dPE and hPE and, despite their existence, cause no anomalous scattering. The assumed values of the parameters are not in obvious conflict with experimental values except possibly for the polydispersity, where we have assumed that the polydispersity $\langle Z\rangle_{wt}/\langle Z\rangle_{num}$ of the deuterated polymer is about 1.2 and the protonated polymer is about 1.02−1.03 while the experimental values[14] are stated to be about 1.1 for both. Whether the GPC (gel permeation chromatography) apparatus, stated[14] to be calibrated for hPE, was equally accurate for dPE polydispersity is unclear. The important caution here is that, for the calculated scattering to be relevant to the experimental data, the experimental systems must consistently have a more polydisperse deuterated polymer than protonated and the experimental differences[14] in polydispersity are consistently too small.

Parenthetically, we note that it would be very convenient for a rationalization of the anomalies if the polymer type present in smaller amount were always to contract, as has been observed in simulations[26,58,59] of what seem to be phase separated systems. But the present calculations involve much smaller χ values and always show expansion relative to Θ values of the dimensions.

2. Packing. Scattering anomalies caused by asymmetries in packing are relevant mainly to polyethylene at large values[15] of f_1, and to polystyrene at both small and large f_1. There is little to discuss, because these asymmetries are due to assumed properties of the partial monomer volumes in the coarse grained thermodynamic model and retain very nearly the same values for macroscopic systems. It is probably much easier to measure these partial monomer volumes than to theorize convincingly about their magnitude,[25] and the numerical results serve only to show the need for such measurements.

B. Theoretical Prospects. It would be fairly straightforward to test the accuracy of the HNC calculations of radial distribution functions based on bare potentials inferred from the phenomenological model, but the validity of the bare potentials presents a more interesting and difficult question. The present theoretical significance of the phenomenological approach is somewhat murky because the distance scale of the coarse grained volume element is undefined except for the requirement that it be much smaller than R_g, and no attempt has been made to test the limits of that requirement or to enforce it. To explore coarse graining on multiple distance scales, the most obvious course would be to simulate melts of Gaussian backbone chains. The simple transformation between monomer coordinates and Rouse modes would probably be sufficiently rapid that the phase space of short wavelength modes could be adequately sampled for a variety of constrained, long wavelength modes (rather than constrained moments of inertia or radii of gyration), and the existence and properties of the free energy density $a(\mathbf{R})$ could then be determined for a sequence of increasing length scales.

C. Experimental Tests. Two sources of anomalous scattering have been considered. To examine the real deviations from Flory−Huggins theory that are manifested in scattering only by systems with asymmetries in molecular weight and polydispersity, it would be useful to examine scattering from melts with substantial and controlled asymmetry in molecular weight. The pseudo-deviations caused by packing asymmetry require simultaneous examination of scattering at the composition extremes and volumes of mixing at all compositions in order to extract the partial monomer volumes and from them the l_k^p.

The theory in this paper develops a quantitative connection between one set of experimental measurements, including particularly the chain lengths and polydispersity, and another set of measurements on the composition dependence of scattering. The connection is based further on specific assumptions about the coarse grained thermodynamic parameters, the compressibility κ_T^0, the energy parameters χ_k and their pressure derivatives, and other properties of the system that are regarded as empirical input, such as the monomer volumes v_t and the bond lengths b_t. The source code for the algorithm that makes the connection is provided in the Supporting Information[16] along with input and output files for all the illustrative calculations and a few others. It is expected that application of the algorithm to other systems of particular interest to the reader will prove straightforward, although attention should be called again to the divergence of HNC iterations for systems with extreme asymmetries of chain length or polydispersity.

Appendix A: Coarse Grained Thermodynamics

We suppose that $a(\mathbf{R}) \equiv a[\phi(\mathbf{R})]$ is a Helmholtz free energy density and in fact regard a as a macroscopic thermodynamic function $a(T, \varphi)$, where the volume fractions φ_i are defined in terms of the numbers of monomers n_i by $\varphi_i = n_i v_i / V_c$. Here V_c is the actual coarse grained volume element and may differ from the volume $V_c^0 \equiv \Sigma_i n_i v_i$ of the pure constituents at the same pressure p. And since p is not initially controlled, the local pressure may vary from one volume element V_c to another, and may differ from the ambient pressure at which the v_i are evaluated. The assumed applicability of macroscopic thermodynamics implies further that $a = A(T, V_c, n)/V_c$, where A is the total Helmholtz free energy of the coarse grained volume element V_c. Of course a is not an ordinary thermodynamic function but an artificial one in which the degrees of freedom are highly constrained; ideally only a small fraction of the internal coordinates of each chain, such as the short wavelength Rouse modes, are actually integrated out in the partition function. Furthermore, polymer chains pass through the walls of V_c, so the assumed form for the Gibbs free energy of mixing ΔG_m at constant p, introduced below, will differ from ordinary ones; it will be chosen to be the excess free energy of mixing in which the entropic contribution from center of mass integrations does not appear. If one wishes to introduce small, solvent molecules into the system, then all of their degrees of freedom would presumably be integrated over and the entropic contribution $k_B T \ln\varphi_0$ to the free energy of mixing would be retained, as in the previous work,[19] but we do not include such terms here.

Regarding notation, only a few symbols such as V_c are given a special notation to indicate their reference to the coarse grained volume element. All of the general equations that precede or do not depend on the particular choice of ΔG_m are applicable to macroscopic volume elements such as the volume of the sample that scatters into a detector, and two such equations are actually used, one for the macroscopic partial monomer volumes (and from them the volume of mixing), and one for the compressibility. The macroscopic properties are all computed from integrals of the radial distribution functions according to equations originally derived by Kirkwood and Buff,[60] but Hill's presentation[61] will be followed. For the macroscopic equations the general notation involving sums over any number of species is necessary, but for the coarse grained volume element the occurrence of those different species is irrelevant because infinitely long chains are supposed to enter and leave the volume element, and each chain provides only one of the two types of monomers that are allowed.

1. Basics. Hill[61] considers the second derivatives of the Helmholtz free energy

$$A_{ij} \equiv \left(\frac{\partial \mu_i}{\partial n_j}\right)_{T,V_c,n} \tag{A1}$$

These derivatives are related as follows to the coefficients $\hat{\epsilon}_{tt'}$ that occur in the bare potentials by

$$a_{ij} = \left(\frac{\partial^2 a}{\partial\varphi_i \partial\varphi_j}\right)_{T,V_c} = \frac{V_c}{v_i v_j} A_{ij} \tag{A2}$$

$$\epsilon_{ij} = \frac{v_0}{k_B T} a_{ij} \tag{A3}$$

$$\epsilon_{ij} = \frac{V_c v_0}{k_B T v_i v_j} A_{ij} \tag{A4}$$

but here the carets are suppressed. The inverse of the matrix $[A]$ affords a connection to fluctuations, scattering, and integrals of the radial distribution functions,

$$([A]^{-1})_{ij} = \left(\frac{\partial n_i}{\partial \mu_j}\right)_{T,V_c,\mu} = \frac{1}{k_B T}\langle \delta n_i \delta n_j \rangle \tag{A5}$$

A transformation from independent variables (T, V, n) to (T, p, n) is introduced through the thermodynamic equalities[61]

$$\left(\frac{\partial p}{\partial n_i}\right)_{T,V_c,n} = \frac{\bar{v}_i}{V_c \kappa_T^c} \tag{A6}$$

$$A_{ij} = \left(\frac{\partial \mu_i}{\partial n_j}\right)_{T,p,n} + \frac{\bar{v}_i \bar{v}_j}{V_c \kappa_T^c} \tag{A7}$$

where κ_T^c is the compressibility of the coarse grained volume element, and we record the identity

$$n_i \left(\frac{\partial \mu_i}{\partial n_j}\right)_{T,p,n} = \left(\frac{\partial (n_i \mu_j)}{\partial n_j}\right)_{T,p,n} - \mu_i \delta_{ij} \tag{A8}$$

from which macroscopic partial monomer volumes and compressibilities can be calculated and related to the fluctuations by taking appropriate sums of eq A7. As previously noted, such formulas are used in the algorithm but are not considered further here; additional discussion and explicit formulas can be found in Friedman[53] and Debenedetti.[62] Note finally that for a one component system $(\partial\mu_1/\partial n_1)_{T,p,n} \equiv 0$ because for a single component μ_1 may be chosen to be a function of p, T.

With eq A7 now available, further analysis can be based on the Gibbs free energy of mixing ΔG_m at constant p. We take

$$\Delta G_m \equiv G - \sum_j n_j \mu_j^0 \tag{A9}$$

to be the excess free energy for the reasons previously stated. $\mu_j^0(T, p)$ is the chemical potential of pure type j

polymer. A standard form[63−65] is used for the expansion of ΔG_m in powers of f_1.

$$\Delta G_m = \frac{k_B T V_c^0}{v_0}\sum_k \chi_k Q_k(f_1) \tag{A10}$$

$$Q_k(f_1) \equiv f_1 f_2 (f_1 - f_2)^k \tag{A11}$$

Q_k is a function of f_1 after the substitution $f_2 = 1 - f_1$. In the program the series is arbitrarily terminated at $k = 1$, but many more terms are sometimes thought necessary for precise measurements on seemingly simple systems.[66] In the FH approximation the series is terminated at $k = 0$, χ_0 is designated χ, and translational entropy terms are added. The coefficients χ_k are functions of (p, T), not of composition, and are in fact the only quantities in ΔG_m that depend on p because we will assume that the two polymers have the same compressibilities, an assumption that makes the f_i independent of p.

The thermodynamic quantities are now obtained by differentiation of ΔG_m. First,

$$\Delta\mu_i \equiv \mu_i - \mu_i^0 = \left(\frac{\partial \Delta G_m}{\partial n_i}\right)_{T,p,n} \tag{A12}$$

from which

$$\Delta\mu_i = \frac{k_B T v_i}{v_0}\sum_k \chi_k \{Q_k + (\delta_{i1} - f_1)Q_k'\} \tag{A13}$$

where $Q_k' \equiv \partial Q_k/\partial f_1$. Another derivative gives

$$\left(\frac{\partial \mu_i}{\partial n_j}\right)_{T,p,n} = \frac{k_B T v_i v_j}{v_0 V_c^0}(\delta_{j1} - f_1)(\delta_{i1} - f_1)\sum_k \chi_k Q_k'' \tag{A14}$$

where $Q_k'' \equiv \partial Q_k'/\partial f_1$.

2. Partial Molar Volumes. Making further use of the assumption that both polymers have the same compressibility so that neither v_i/v_0 or Q_k depend on p, and the thermodynamic equaility $\bar{v}_i = (\partial\mu_i/\partial p)_{T,n}$, one finds

$$\bar{v}_i = v_i + v_i \sum_k l_k^p [Q_k + (\delta_{i1} - f_1)Q_k'] \tag{A15}$$

where

$$l_k^p \equiv \frac{k_B T}{v_0}\left(\frac{\partial \chi_k}{\partial p}\right)_{T,n} \tag{A16}$$

3. Compressibility. The coarse grained volume is

$$V_c = \sum_i n_i \bar{v}_i$$

$$V_c = \sum_i n_i v_i \{1 + \sum_k l_k^p [Q_k + (\delta_{i1} - f_1)Q_k']\} \tag{A17}$$

and

$$\frac{\partial V_c}{\partial p} = \sum_i n_i \frac{\partial v_i}{\partial p}\{1 + \sum_k l_k^p [Q_k + (\delta_{i1} - f_1)Q_k']\} + \sum_i n_i v_i \{\sum_k l_k^{p\prime} [Q_k + (\delta_{i1} - f_1)Q'_k]\} \tag{A18}$$

where $l_k^{p\prime} \equiv \partial l_k/\partial p$. We assume that the $l_k^{p\prime}$ are negligible, so

$$\frac{\partial V_c}{\partial p} = -\kappa_T^0 \sum_i n_i v_i \{1 + \sum_k l_k^p [Q_k + (\delta_{i1} - f_1)Q_k']\} \tag{A19}$$

where κ_T^0 is, by previous assumption, the compressibility of either of the pure components. It follows that

$$\kappa_T^c = \kappa_T^0 \tag{A20}$$

4. Coefficients. Returning to eqs A7 and A14, we have

$$A_{ij} = \frac{\bar{v}_i \bar{v}_j}{V_c \kappa_T^c} + \frac{k_B T v_i v_j}{v_0 V_c^0}(\delta_{j1} - f_1)(\delta_{i1} - f_1)\sum_k \chi_k Q_k'' \tag{A21}$$

Then eq A4 for ϵ_{ij} gives

$$\epsilon_{ij} = \epsilon_c \frac{\bar{v}_i \bar{v}_j}{v_i v_j} + \frac{V_c}{V_c^0}(\delta_{j1} - f_1)(\delta_{i1} - f_1)\sum_k \chi_k Q_k'' \tag{A22}$$

where

$$\epsilon_c \equiv \frac{v_0}{k_B T \kappa_T^c} \tag{A23}$$

Specifically

$$\epsilon_{11} = \epsilon_c \left(\frac{\bar{v}_1}{v_1}\right)^2 - \frac{V_c}{V_c^0} f_2{}^2 S_\kappa \tag{A24}$$

$$\epsilon_{22} = \epsilon_c \left(\frac{\bar{v}_2}{v_2}\right)^2 - \frac{V_c}{V_c^0} f_1{}^2 S_\kappa \tag{A25}$$

$$\epsilon_{12} = \epsilon_c \frac{\bar{v}_1 \bar{v}_2}{v_1 v_2} + \frac{V_c}{V_c^0} f_1 f_2 S_\kappa = \epsilon_{21} \tag{A26}$$

where

$$S_\kappa \equiv -\sum_k \chi_k Q_k'' \tag{A27}$$

It follows that

$$\epsilon_{12}{}^2 - \epsilon_{11}\epsilon_{22} = \epsilon_c \left(\frac{V_c}{V_c^0}\right)^3 S_\kappa \tag{A28}$$

and the parameters χ^{FH}, ϵ, and r_ϵ defined in eqs 2.33−2.35, respectively, can be readily evaluated. It should be noted that while χ^{FH} is proportional to S_κ, the parameters ϵ and r_ϵ are virtually independent of S_κ, and the quantity r_ϵ referred to as a measure of the relative packing energies of the two types of polymer, is basically determined by their partial monomer volumes according

to eqs A24 and A25, for relevant values of κ_T^0 and other coarse grained parameters, which make $S_\kappa \ll 1$ and $\epsilon_c \gg 1$.

Supporting Information Available: Additional documentation, application runs with timings, input/output files, and the source code. This material is available free of charge via the Internet at http://pubs.acs.org.

References and Notes

(1) Crist, B. *J. Polym. Sci., Part B: Polym. Phys.* **1997**, *35*, 2889.
(2) Crist, B. *Macromolecules* **1998**, *31*, 5853.
(3) Melenkevitz, J.; Crist, B.; Kumar, S. K. *Macromolecules* **2000**, *33*, 6869.
(4) General references to deuterated or natural polymers should be understood in this paper to refer to the polymers with larger or smaller scattering lengths, respectively.
(5) In this work $I(q)$ is defined by eq 4.1, in the section on Scattering, and is presumed to be the quantity reported in experimental papers. Equation 1.1 is regarded as a mere definition of X_{ns} that follows experimental practice, but the extrapolation to $q = 0$ does not always seem devoid of theoretical premises.
(6) The units of $I(q)$ are the same as those of α^2/v, see eq 4.1, thus being $Å^{-1}$ for neutron scattering.
(7) The word type is used in place of thermodynamic component with a similar but more limited meaning. Each type of polymer may have a distribution of molecular weights and internal states, but all such polymeric species assigned to a single polymer type are presumed to be composed of a single monomer type. The types are labeled with subscripts t and t' and the more numerous chemical species with subscripts s and u. For some quantities, such as v_s, v_t or Z_s, Z_t, the subscripts and/or context bear the whole burden of distinguishing between species and types. Numerical subscripts, such as v_1, Z_1, always indicate a reference to types rather than species.
(8) Koningsveld, R.; Stockmayer, W. H.; Nies, E. *Polymer Phase Diagrams;* Oxford University Press: Oxford, England, 2001.
(9) Akcasu, A. Z.; Tombakoglu, M. *Macromolecules* **1990**, *23*, 607.
(10) Benoit, H.; Benmouna, M.; Li Wu, W. *Macromolecules* **1990**, *23*, 1511.
(11) de Gennes, P. G. *Scaling Concepts in Polymer Physics;* Cornell University Press: New York, 1979.
(12) Balsara, N. P.; Fetters, L. J.; Hadjichristidis, N.; Lohse, D. J.; Han, C. C.; Graessley, W. W.; Krishnamoorti, R. *Macromolecules* **1992**, *25*, 6137.
(13) Balsara, N. P.; Lohse, D. J.; Graessley, W. W.; Krishnamoorti, R. *J. Chem. Phys.* **1994**, *100*, 3905.
(14) Londono, J. D.; Narten, A. H.; Wignall, G. D.; Honnell, K. G.; Hsieh, E. T.; Johnson, T. W.; Bates, F. S. *Macromolecules* **1994**, *27*, 2864.
(15) The evidence for scattering anomalies seems less persuasive at large f_1 because of large subtractions for background; for example, Londono et al.[14] subtract 90% of the scattering as background at $f_1 = 0.9$.
(16) See paragraph at end of paper for information about the Supporting Infomation.
(17) Yamakawa, H. *Modern Theory of Polymer Solutions*; Harper & Row Publishers: New York, 1971.
(18) Rowlinson, J. S.; Widom, B. *Molecular Theory of Capillarity;* Oxford University Press: Oxford, England, 1982.
(19) Fixman, M. *J. Chem. Phys.* **1961**, *35*, 889.
(20) Taylor, J. K.; Debenedetti, P. G.; Graessley, W. W.; Kumar, S. K. *Macromolecules* **1996**, *29*, 764.
(21) Joanny, J. F.; Benoit, H. *Macromolecules* **1997**, *30*, 3704. In Joanny and Benoit, v_s is a partial molecular volume in the mixture and is in principle dependent on composition. We use $\bar{v}_s$ and $\bar{V}_s$ for partial volumes in the mixture and v_s for partial monomer volumes of pure polymers.
(22) Krishnamoorti, R.; Graessley, W. W.; Balsara, N. P.; Lohse, D. J. *J. Chem. Phys.* **1994**, *100*, 3894.
(23) Beiner, M.; Fytas, G.; Meier, G.; Kumar, S. K. *Phys. Rev. Lett.* **1998**, *81*, 594.
(24) Beiner, M.; Fytas, G.; Meier, G.; Kumar, S. *J. Chem. Phys.* **2002**, *116*, 1185.
(25) Krishnamoorti et al.[22] report negligible volumes of mixing for mixtures of protonated and partially deuterated polybutadienes at 23 °C, but this information is not useful because the significant anomalous scattering in the composition extremes was reported for mixtures studied at much higher temperatures. Beiner et al.[23] report large relative volumes of mixing, with magnitude ranging between −0.026 and +0.016 depending on temperature and composition, for blends of poly(ethylmethylsiloxane) and poly(dimethylsiloxane), but they reported[24] the (light) scattering only at $f_1 = 0.5$. Given the major contribution to scattering anomalies caused by composition dependent partial monomer volumes, nothing less than a careful study of the composition dependence of volumes of mixing for the actual scattering samples, conditions, and preparative methods would provide sufficient grounds at the present time to rule out their significance.
(26) Murat, M.; Kremer, K. *J. Chem. Phys.* **1998**, *108*, 4340.
(27) Eurich, F.; Maass, P. *J. Chem. Phys.* **2001**, *114*, 7655. We have used the approximate probability distribution provided by these authors for the radius of gyration.
(28) Eurich, F.; Maass, P.; Baschnagel, J. *J. Chem. Phys.* **2001**, *117*, 4564.
(29) Lang, A.; Likos, C. N.; Watzlawek, M.; Löwen, H. *J. Phys.: Condens. Matter* **2000**, *12*, 5087.
(30) Bates, F..; Fredrickson, G. I. *Macromolecules* **1994**, *27*, 1065.
(31) Fredrickson, G. H.; Liu, A. J.; Bates, F. S. *Macromolecules* **1994**, *27*, 2503.
(32) Fredrickson, G. H.; Liu, A. J. *J. Polym. Sci., Part B: Polym. Phys.* **1995**, *33*, 1203.
(33) Buta, D.; Freed, K. F.; Szleifer, I. *J. Chem. Phys.* **2001**, *114*, 1424.
(34) Vlahos, C.; Kosmas, M. *Polymer* **2003**, *44*, 503.
(35) Lipson, J. E. G.; Tambasco, M.; Willets, K. A.; Higgins, J. S. *Macromolecules* **2003**, *36*, 2977.
(36) Hu, W.; Frenkel, D.; Mathot, V. B. F. *J. Chem. Phys.* **2003**, *118*, 10343.
(37) Tsige, M.; Curro, J. G.;; Grest, G. S.; McCoy, J. D. *Macromolecules* **2003**, *36*, 2158.
(38) Patil, R.; Schweizer, K. S.; Chang, T.-M. *Macromolecules* **2003**, *36*, 2544.
(39) Sollich, P. *J. Phys.: Condens. Matter* **2002**, *14*, R79.
(40) Fredrickson, G. H.; Sides, S. W. *Macromolecules* **2003**, *36*, 5415.
(41) Wang, Z.-G. *J. Chem. Phys.* **2002**, *117*, 481.
(42) Yethiraj, A.; Fynewever, H.; Shew, C.-Y. *J. Chem. Phys.* **2001**, *114*, 4323.
(43) Berg, L.; Painter, P. *J. Polym. Sci., Part B: Polym. Phys.* **2003**, *41*, 2923.
(44) Kumar, S. K.; Veytsman, B. A.; Maranas, J. K.; Crist, B. *Phys. Rev. Lett.* **1997**, *79*, 2265.
(45) Taylor-Maranas, J. K.; Debenedetti, P. G.; Graessley, W. W.; Kumar, S. K. *Macromolecules* **1997**, *30*, 2265.
(46) Ma, S.-K. *Modern Theory of Critical Phenomena;* W. A. Benjamin, Inc.: Reading, MA, 1976.
(47) Fredrickson, G. H.; Ganesan, V.; Drolet, F. *Macromolecules* **2002**, *35*, 16.
(48) The restriction to one or two chemical types applies only to the input and output routines, and could be easily removed if sufficient knowledge about the off-diagonal elements of ϵ_{su} were available to make the calculations worthwhile.
(49) Fixman, M. *J. Chem. Phys.* **1962**, *36*, 3123.
(50) Theodorou, D. N.; Suter, U. W. *Macromolecules* **1985**, *18*, 1206.
(51) Janszen, H. W. H. M.; Tervoort, T. A.; Cifra, P. *Macromolecules* **1996**, *29*, 5678.
(52) Fixman, M. *J. Chem. Phys.* **1962**, *36*, 306.
(53) Friedman, H. L. *A course in statistical mechanics;* Prentice Hall: Englewood Cliffs, NJ, 1985.
(54) Friedman, H. L.; Dale, W. D. T. Electrolyte solutions at equilibrium. In *Statistical Mechanics, Part A: Equilibrium Techniques*; Berne, B. J., Ed.; Plenum Press: New York, 1977.
(55) Rossky, P. J.; Dale, W. D. T. *J. Chem. Phys.* **1980**, *73*, 2457.
(56) Much larger deviations in the correlation hole, up to 5 or 10%, occur for melts with asymmetric packing, the magnitude depending on the compressibility.
(57) More precisely, the anomalies due to packing asymmetry are made to become very small, and nearly invisible in the figures, by the use of β^Y instead of β^X. A residual anomaly remains if the compressibility is finite, as discussed in the Introduction. An unfortunate choice of scattering lengths could reduce the scattering from composition fluctuations to values comparable with scattering from density fluctuations, and greatly magnify the anomaly, but such systems are not likely to be the subject of experimental study.
(58) Sariban, A.; Binder, K. *Macromolecules* **1988**, *21*, 711.
(59) Müller, M. *Macromolecules* **1998**, *31*, 9044.

(60) Kirkwood, J. G.; Buff, F. P. *J. Chem. Phys.* **1951**, *19*, 774.
(61) Hill, T. L. *Statistical Mechanics;* McGraw-Hill Book Company, Inc.: New York, 1956. See the discussion of composition fluctuations on pp 113ff, Section 21.
(62) Debenedetti, P. G. *J. Chem. Phys.* **1987**, *86*, 7126.
(63) Rowlinson, J. S.; Swinton, F. L. *Liquids and Liquid Mixtures*, 3rd ed.; Butterworth: London, 1982.
(64) Hildebrand, J. H.; Scott, R. L. *Solubility of Nonelectrolytes*, 3rd ed.; Reinhold Publishing Corporation: New York, 1950.
(65) Luszczyk, M.; Hook, W. A. V. *Macromolecules* **1996**, *29*, 6612.
(66) Dutta-Choudhury, M. K.; Dessauges, G.; Hook, W. A. V. *J. Phys. Chem.* **1982**, *86*, 4068.

MA049646S